Cell. Mol. Life Sci. (2017) 74:571–577
DOI 10.1007/s00018-016-2424-6

Cellular and Molecular Life Sciences

ERRATUM

Erratum to: Protease-activated-receptor-2 affects protease-activated-receptor-1-driven breast cancer

Mohammad Jaber[1] · Miriam Maoz[1] · Arun Kancharla[1] · Daniel Agranovich[1] · Tamar Peretz[1] · Sorina Grisaru-Granovsky[2] · Beatrice Uziely[1] · Rachel Bar-Shavit[1]

Published online: 30 November 2016

Erratum to: Cell. Mol. Life Sci. (2014) 71:2517–2533
DOI 10.1007/s00018-013-1498-7

In the published article, duplicated or inverted gel sections had been used in the Figs. 1Ai, Aii, D, 2Aii, 4B and 6C. In agreement with the Editor-in-Chief the experiments were repeated and the same results obtained. The primary data from the repeated experiments can be found below.

The online version of the original article can be found under doi:10.1007/s00018-013-1498-7.

✉ Rachel Bar-Shavit
Rachelbar@ekmd.huji.ac.il

[1] Sharett-Institute of Oncology, Hadassah-Hebrew University Medical Center, POB 12000, 91120 Jerusalem, Israel

[2] Department of Obstetrics and Gynecology, Shaare-Zedek and Hadassah-Hebrew University Medical Centers, POB 12000, 1120 Jerusalem, Israel

Silencing of *hPar2* inhibits the co-IP of Etk/Bmx with PAR_1 C-tail

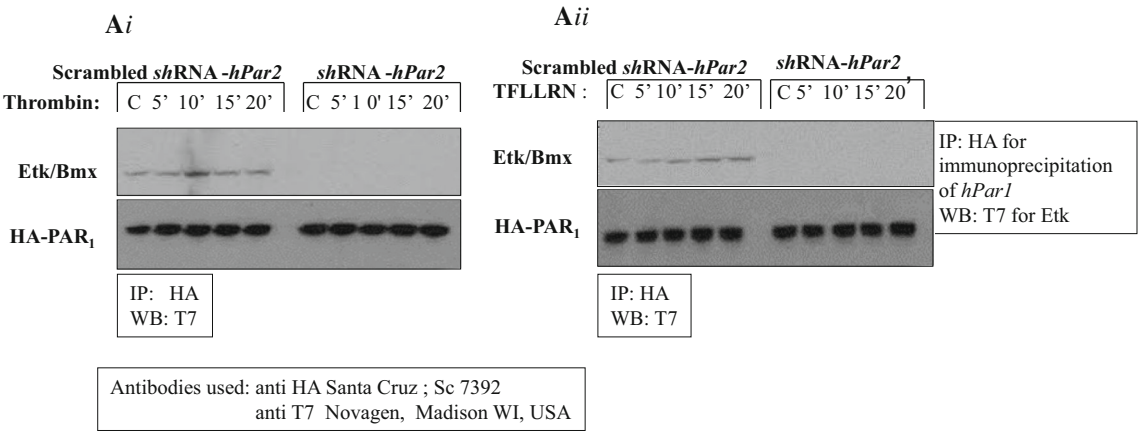

Antibodies used: anti HA Santa Cruz ; Sc 7392
anti T7 Novagen, Madison WI, USA

B Silencing of *hPar2* inhibits the co-IP of Akt with PAR_1 C-tail and its phosphorylation

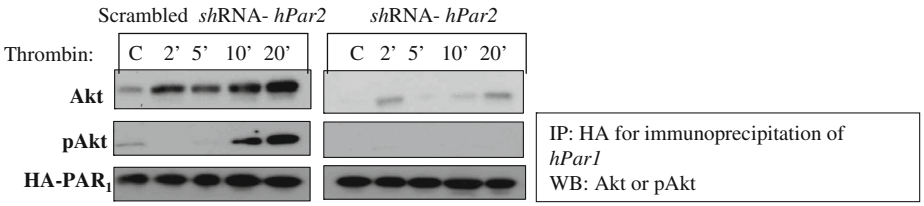

C Levels of transfection and silencing in the MCF-7 clones

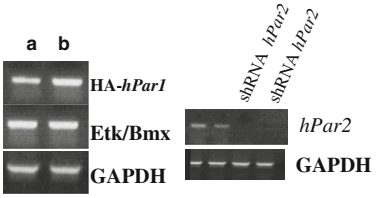

D **Silencing of *hPar2* inhibits selectively PAR_1 activated co-association of Akt with PAR_1 C-tail in MDA-MB-231 cells**

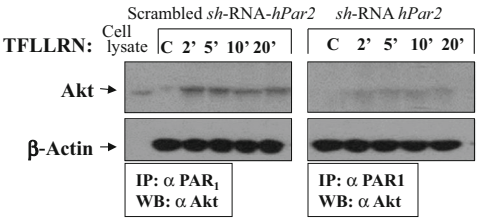

Antibodies used: anti PAR_1 BioLegend clone N2-11# 659102 San Diego, Ca
anti Akt Cell Signaling #9272
anti β-actin Sigma A5441

Explanatory note: Total cell lysate is not part of the immunoprecipitation (IP) assay. It serves as an internal indicator for the size of Akt on the gel.

◀**Fig. 1** Silencing of *hPar2* inhibits association of key signaling partners with the PAR_1 C-tail. **A***i* MCF7 cells stably over-expressing HA-*hPar1* and T7-Etk/Bmx were infected with a lentiviral vector driving either *sh*RNA- *hPar2* expression or a scrambled *sh*RNA-*hPar2* and cultured with or without thrombin activation (1 U/ml) (**A***i*) or the PAR_1 selective ligand, TFLLRN (100 μM) (**A***ii*). Cell lysates were collected at the indicated times and immunoprecipitated using anti-HA antibodies. Immunoprecipitates were separated on SDS-PAGE and Western blotted with anti-T7 antibody to detect T-7 tagged Etk/Bmx. Maximal association of Etk/Bmx is seen after 10 min of thrombin treatment in cells without *hPar2* silencing (scrambled *sh*RNA-*hPar2*); but is not detectable in cells infected with *shRNA-Par2*. A specific, Etk/Bmx is seen associated after 5′, 10′, 15′, and 20 min following TFLLRN activation in cells expressing both HA-*hPar1* and endogenous *hPar2* (scrambled *sh*RNA-*hPar2*). In-contrast, the Etk/Bmx association is not detected in the presence of *shRNA-hPar2*. **B** Silencing *hPar2* inhibits thrombin-induced association between PAR_1 and Akt. MCF7 clones overexpressing HA-*hPar1*, with *sh*RNA *hPar2* silencing (*right*), or scrambled *sh*RNA *hPar2* (*left*), were treated with thrombin for the indicated times. Cell lysates were immunoprecipitated with anti-HA to precipitate HA-PAR_1 and analyzed by Western blot with anti-Akt antibodies, followed by antibodies to phosphorylated Akt (pAkt). HA-PAR_1 serves as a loading control. **C** PAR_2 expression in the MCF7 clone (expressing *hPar1*, *hPar2*, and *etk/bmx*) with and without *sh*RNA silencing as compared with a housekeeping gene GAPDH. **D** Silencing *hPar2* inhibits TFLLRN PAR_1 activation in MDA-MB-231 cells. MDA-MB-231 cells expressing high endogenous levels of both PAR_1 and PAR_2 show a similar pattern (to MCF7 cells) of selective PAR_1 inhibition in the presence of *sh*-RNA *hPar2*. TFLLRN activation induces the co-IP between PAR_1 and Akt immediately after 2′, 5′, 10′, and 20′ activation (scrambled *sh*-RNA *hPar2*). In the presence of *sh*-RNA *hPar2*, this association is markedly inhibited. β-actin serves as a loading control

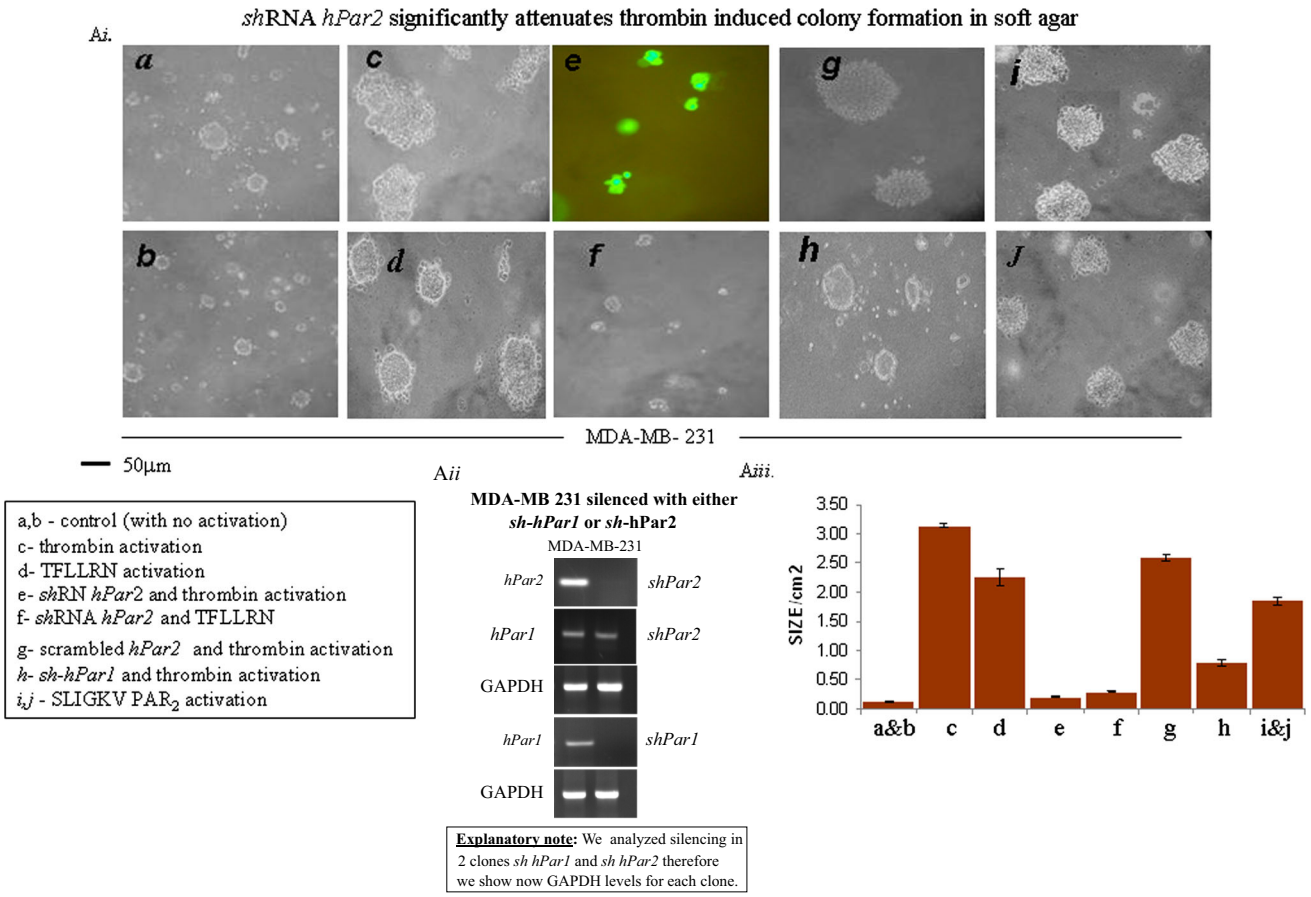
shRNA hPar2 significantly attenuates thrombin induced colony formation in soft agar
Ai.
a
c
e
g
i
b
d
f
h
J
MDA-MB- 231
50µm
a,b - control (with no activation)
c- thrombin activation
d- TFLLRN activation
e- shRN hPar2 and thrombin activation
f- shRNA hPar2 and TFLLRN
g- scrambled hPar2 and thrombin activation
h- sh-hPar1 and thrombin activation
i,j - SLIGKV PAR2 activation
Aii
MDA-MB 231 silenced with either
sh-hPar1 or sh-hPar2
MDA-MB-231
hPar2
shPar2
hPar1
shPar2
GAPDH
hPar1
shPar1
GAPDH
Explanatory note: We analyzed silencing in 2 clones sh hPar1 and sh hPar2 therefore we show now GAPDH levels for each clone.
Aiii.
SIZE/cm2
3.50
3.00
2.50
2.00
1.50
1.00
0.50
0.00
a&b
c
d
e
f
g
h
i&j

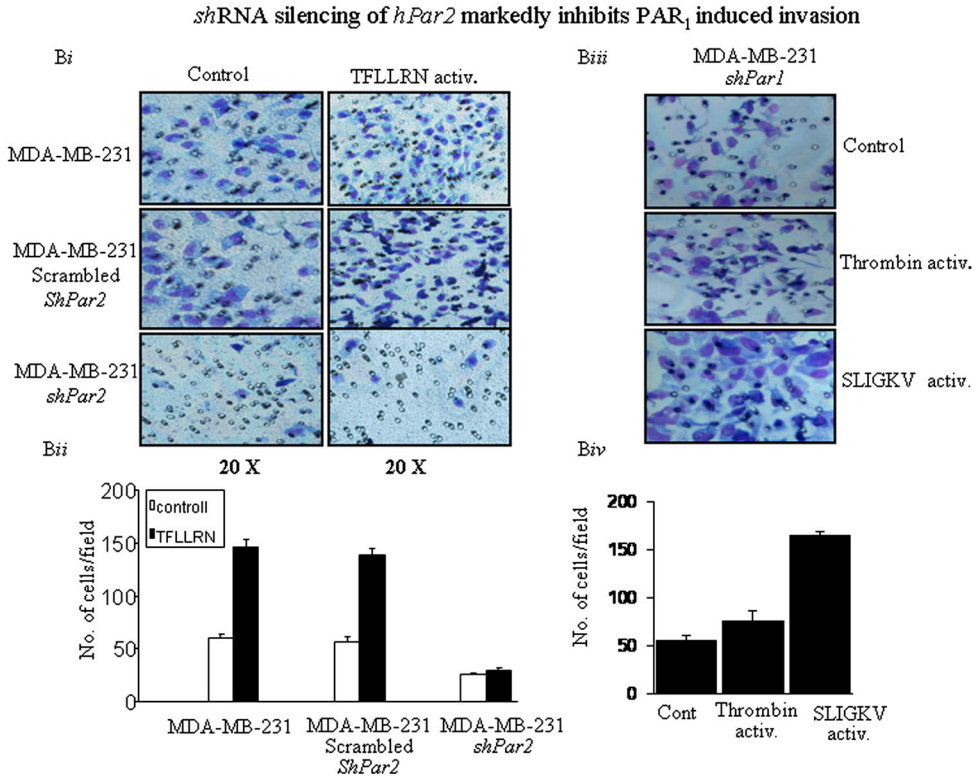
shRNA silencing of hPar2 markedly inhibits PAR1 induced invasion
Bi
Control
TFLLRN activ.
MDA-MB-231
MDA-MB-231
Scrambled
ShPar2
MDA-MB-231
shPar2
Biii
MDA-MB-231
shPar1
Control
Thrombin activ.
SLIGKV activ.
Bii
20 X
20 X
200
150
100
50
0
No. of cells/field
controll
TFLLRN
MDA-MB-231
MDA-MB-231
Scrambled
ShPar2
MDA-MB-231
shPar2
Biv
200
150
100
50
0
No. of cells/field
Cont
Thrombin
activ.
SLIGKV
activ.

◀**Fig. 2** **A***i* Silencing *hPar2* in a breast cancer cell line inhibits thrombin- or TFLLRNPNDK-induced colony formation in soft agar. 5×10^3 MDA-MB-231 cells, either uninfected (*a*, *b*) or infected with virus expressing *sh*RNA-GFP-*hPar2* (*e, f*), were plated in soft agar and activated by thrombin (*e*) or TFLLRNPNDK (*f*). Uninfected cells were treated with thrombin (*c*) or TFLLRN (*d*) as also with SLIGKV (**i**, **j**). Controls of either scrambled *sh*RNA *hPar2* with thrombin activation (*g*) and *sh*RNA *hPar1* with thrombin activation (*h*) were shown as well. After 12 days, live images were collected using a Zeiss microscope at ×20 magnification. In uninfected cells, large colonies formed following treatment with either thrombin (*c*) and somewhat smaller with TFLLRNPNDK (*d*). MDA-MB-231 cells infected with *sh*-GFP-*hPar2* formed only very small colonies after thrombin (*e*) or TFLLRNPNDK (*f*) treatment. Cells containing *sh-hPar2* are visualized by GFP fluorescence (*e*). The colonies formed under different conditions were compared with control non-activated, non-treated cells (control; *a, b*). The colonies formed in the presence of *sh*RNA-*hPar1* and after thrombin activation is significantly smaller (panel *h*) than colonies formed after thrombin activation (*c*). Scrambled *sh*RNA-*hPar2* had no effect on the colonies formed (panel *g*). Comparable colony size is obtained by SLIGKV PAR_2 activation (*i, j*) as found by TFLLRNPNDK (*d*). Images shown are representative of three independent experiments. **A***ii* RT-PCR analysis of *hPar1* and *hPar2* mRNA expression before and after *sh*RNA silencing. GAPDH levels were analyzed as a control. **A***iii* Histogram shows mean ± SE of triplicate values from three independent experiments. Post hoc evaluation of multiple comparison (ANOVA Tukey HSD) showed a *p* value of 0.004 within groups. The mean difference is significant at the 0.05 level. For ANOVA evaluation we used IBM SPSS 20.0 software. **B***i* Silencing *hPar2* in MDA-MB-231 cells inhibits TFLLRN PAR_1 invasion. Matrigel invasion in the presence of *sh*RNA-*hPar2*-infected cells as compared with scrambled *sh*RNA. While TFLLRN specific activation of PAR_1 induces Matrigel invasion in MDA-MB-231 cells, this was attenuated in the presence of *sh*RNA-*hPar2*-infected cells. In-contrast, no effect was observed when a scrambled *sh*RNA was utilized to infect the cells, demonstrating a markedly induced Matrigel invasion similar to non-treated activated parental MDA-MB-231 cells. **B***ii* Histograms represents quantification of the cells/HPF invaded the Matrigel layer. Unpaired Student's *t* test was used. This experiment is a representative of three independent experiments performed in triplicates. **B***iii* Silencing *hPar1* in MDA-MB-231 cells did mot inhibit PAR_2 function. In MDA-MB-231 cells silenced for *hPar1*, thrombin activation resulted with a low level of Matrigel invasion. In-contrast, SLIGKV PAR_2 activation under conditions of *sh-hPar1* silencing, resulted with potent Matrigel invasion. **B***iv* Histograms represents quantification of the cells/HPF invaded the Matrigel layer in *sh*RNA *hPar1* silenced cells. Unpaired Student's *t* test was used. This experiment is a representative of three independent experiments performed in triplicates

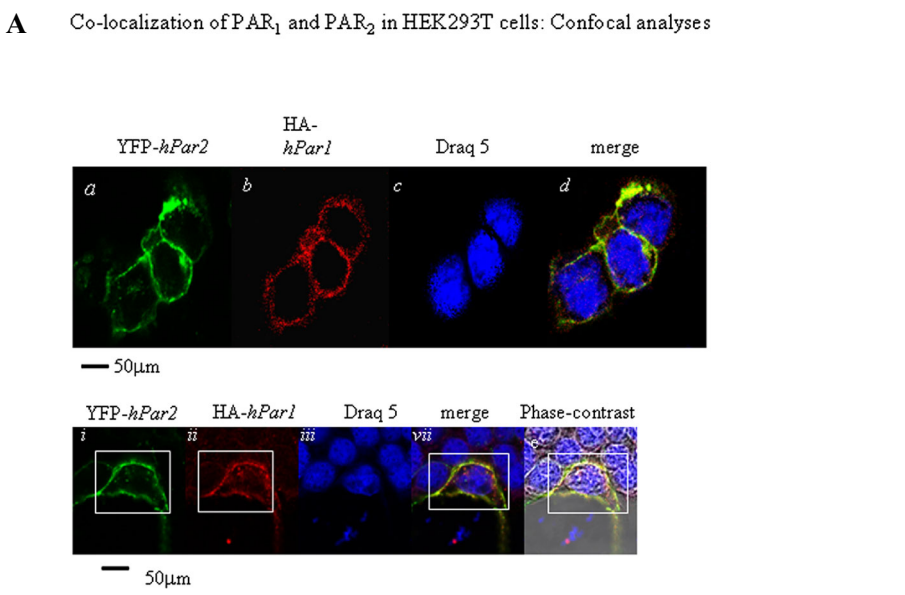

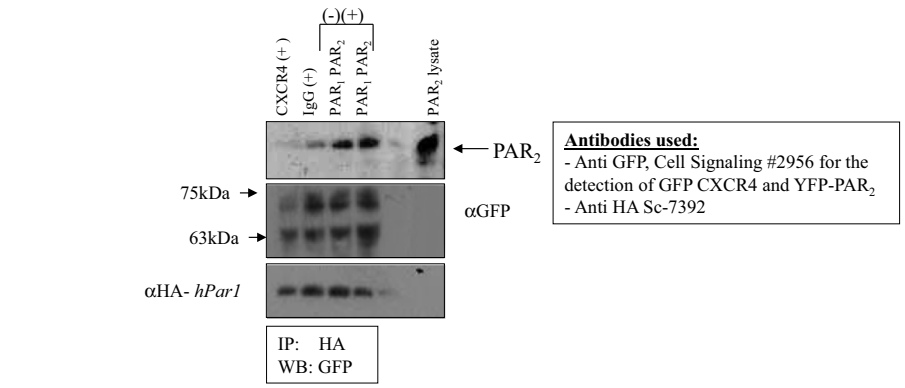

Explanatory note: HEK293 cells were transfected with: YFP-*hPar2,* HA-*hPar1* and GFP-CXCR4 plasmids. The size of CXCR4 is ~39kDa, GFP is 27 kDa resulting with total size of ~**66 kDa.** The size of PAR_2 plus YFP (26kDa), as seen in the original gel (see slide number 11) is approximately **63kDa**. Under the gel condition used in the repeated experiment we could not detect the ~3kDa difference. The GFP detected two band. We refer to the lower band as both CXCR4 –GFP and PAR_2-YFP. The upper band may detect higher forms of PAR_2 (e.g., possibly a glycosylated form).

Fig. 4 Co-localization of PAR_1 and PAR_2. **A** Confocal immunofluorescence analysis. HEK-293T cells were transfected with both HA-*hPar1* and YFP-*hPar2*. After 24 h, the cells were serum deprived for an additional 24 h then activated with thrombin for 5 min followed by fixation with cold methanol. PAR_2 was visualized by direct fluorescence (*a*) and PAR_1 was visualized by immunostaining with anti HA-antibodies followed by Cy3-conjugated IgG secondary antibodies (*b*). Merge staining for both PAR_1 and PAR_2 revealed co-localization confined to the cell membrane (*d*). For reference, staining of cell nuclei with Draq5 is shown (*c*). The *bottom panel* highlights staining in one cell exhibiting the expression of YFP-*hPar2* and HA-*hPar1* on the cell membrane prior to activation (*i, ii*). Significant co-localization recapitulated by merge fluorescence is observed following five minutes thrombin activation (*iv*). This is detected as compared with cell nuclei staining (*iii*) and phase-contract analysis (*v*). The percent of positive cells for HA-*hPar1* was 58 % ± 1.2 and for YFP-*hPar2* were 55 % ± 1.86; PAR_1-PAR_2 merge was observed in 45 % ± 2.1. **B** PAR_1 and PAR_2 co-immunoprecipitate. HEK 293T cells expressing either HA-*hPar1*, YFP-*hPar2* or GFP-CXCR4 were treated with thrombin for 10 min and lysed. Cell lysates were then immunoprecipitated before (−) and after (+) thrombin activation by anti HA or IgG, resolved by SDS-PAGE and immunoblotted as indicated (by anti-GFP). While no specific complex is formed when CXCR4 and PAR_1 were co-IP (following 10-min thrombin activation), a specific complex is observed between PAR_1 and PAR_2 following activation. No specific band is seen when IgG were applied in the immunoprecipitation assay. Expression of CXCR4, PAR_2 (as indicated by anti-GFP, *first lane*), and PAR_1 (as shown by anti-HA) were shown as controls for transfection efficiency. The figure shown is a representative of three independent experiments

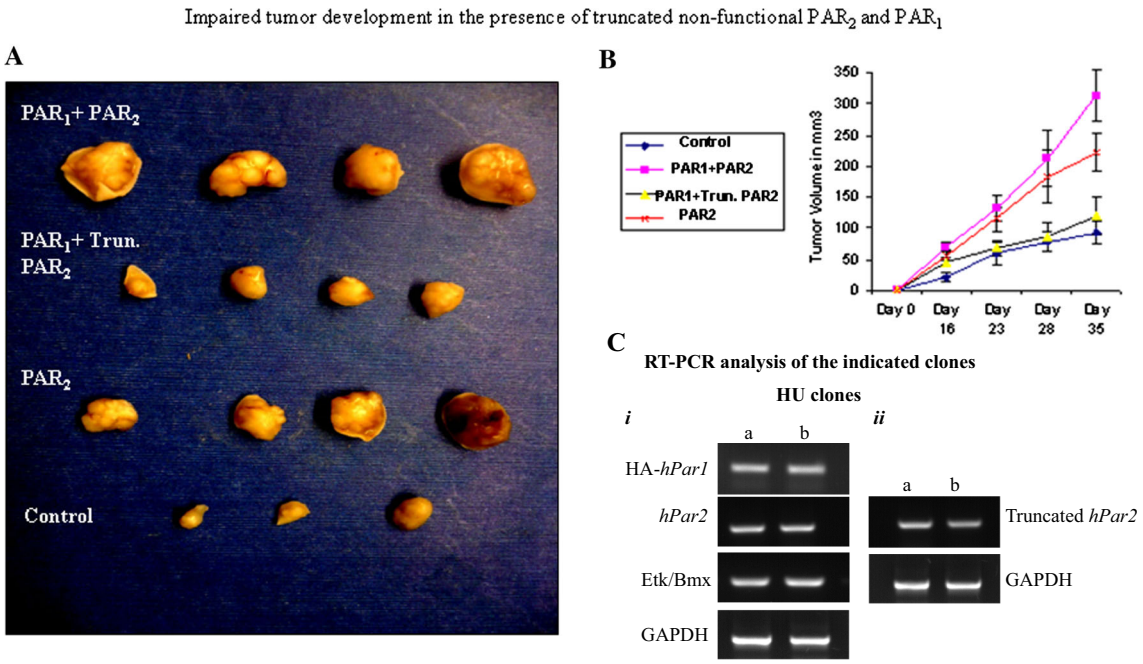

Fig. 6 Impaired tumor development in the presence of PAR_1 and truncated PAR_2. Stable clones of HU cells expressing either *hPar2* or *hPar1* and *hPar2*, or *hPar1* and truncated *hPar2* were injected subcutaneously into nude mice (2×10^6 cell/mouse). Parental non-transfected HU cells were used as a control. **A** Tumor morphological appearance. Mice injected either with *hPar1* and *hPar2 or hPar2* developed tumors at the sites of injection. In-contrast, mice inoculated with *wt hPar1* and a truncated form of *hPar2* did not develop or developed very little tumors (*a*). By the end of the experiment (e.g., 35 days) the mice were killed and the tumors were excised, measured, and weighed ($n = 4$/per group). **B** Mouse tumor growth curve in nude mice. Tumors were excised, weighed and measured at the indicated times and tumor volume (mm^3) was calculated. *Error bars* show SD; * indicates $p < 0.006$. Data shown are representative of three experiments performed. **C***i, ii* RT-PCR analyses of the indicated clones (*a* and *b*; two different clones) show the expression of PAR_1 and PAR_2, truncated PAR_2 and the prime signal protein Etk/Bmx